Effect of Axial Inhomogeneity on Solitons Near the Zero Dispersion Point

P. K. A. WAI, C. R. MENYUK, H. H. CHEN, AND Y. C. LEE

Abstract—**It is shown both numerically and analytically that solitons emerge from initial pulses in the neighborhood of the zero dispersion point even when axial inhomogeneity causes large fluctuations in the zero dispersion point's location. The criterion for soliton propagation in this regime is that the correlation length of the variations is much shorter than the second-order and the third-order dispersion lengths.**

I. Introduction

In the linear regime, the maximum bit rate which can be transmitted over a single-mode optical fiber is limited by dispersion. If we consider a pure silica fiber with a length of 30 km and propagation at the minimum loss point $\lambda = 1.55$ μm, we find that dispersion limits the bit rate to about 10 Gbits. At the so-called "zero dispersion point" where second-order dispersion is zero, the linear dispersion is minimized; it is not really zero because the third-order dispersion is nonzero. Nonetheless, the maximum obtainable bit rate increases to roughly 300 Gbits. Unfortunately, this approach suffers from the drawback that deviations away from the zero dispersion point of only 1 percent will degrade the bit rate by a factor of ten, and the zero dispersion point always shifts along the fiber due to variations in the core size. Another approach which has been proposed is to make use of the Kerr effect in the anomalous dispersion regime to produce solitons, nonlinear pulses which propagate without dispersive broadening [1]. This idea, while quite promising, suffers at present from the drawback that quite substantial power, on the order of 1 W peak power for a 5 ps pulse, is needed to produce a soliton. While this peak power can be substantially reduced in specially manufactured fiber, the doping process which produces this fiber will lead to far higher attenuation loss. At the same time, the soliton scheme is quite robust since solitons will propagate whenever $\lambda \gtrsim 1.3$ μm. Moreover, this scheme lends itself naturally to the use of amplifiers rather than repeaters [2]–[4].

Recently, we have proposed a scheme which combines the low power requirement of propagation at the zero dispersion point with the robustness of the soliton approach [5]. If a pulse is launched at or near the zero dispersion point, then the nonlinear Schrödinger equation which has been used to model phenomena in the anomalous dispersion regime is no longer valid. Nonetheless, a soliton (or more precisely, a solitary wave) is created anyway. Moreover, this soliton has a peak power which is substantially lower than that for solitons in the anomalous dispersion regime, putting the use of laser diodes within reach. When the soliton forms, the nonlinearity downshifts its center frequency into the anomalous dispersion regime. As a consequence, the soliton is quite robust. At the same time that the soliton forms, a substantial fraction of the initial pulse power will, in general, go into a dispersive wave component. This fraction is quite sensitive to the initial central frequency of the launched pulse and is generally substantial. When the initial central frequency is exactly at the zero dispersion point, this fraction is about 40 percent. However, the dispersive wave component is upshifted by the nonlinearity into the normal dispersion regime, so that there is a clear frequency separation between the soliton and the dispersive waves. Hence, the latter can, in principle, be removed by filtering the signal.

In previous work [5], we concentrate on demonstrating that a soliton forms when a pulse is launched at or near the zero dispersion point, ignoring the response of the soliton to variations in the zero dispersion point along the fiber length due to axial inhomogeneity. The core diameter of a step-index fiber typically has a tolerance of 1 percent [6]. While the amount of the fluctuation is small and has little effect on soliton propagation in the anomalous dispersion regime, it can have a significant effect in the new proposed scheme. The zero dispersion point is the result of a balance between the material dispersion and the waveguide dispersion. The material dispersion is independent of the fiber design, but the waveguide dispersion is sensitive to variations of the fiber parameters. Small deviations from the prescribed value would shift the balance such that a pulse launched at the zero dispersion wavelength at one point of the fiber would encounter strong chromatic dispersion later. In this paper, we show both analytically and numerically that within the physically important parameter range where the correlation length of the axial variations is much shorter than the second-order and the third-order dispersion length, soliton propagation is possible even for large amplitude of fluctuation in the second-order dispersion. Physically, the second-order dispersion varies so fast that the pulse cannot respond to it. Its evolution is therefore governed by the weaker third-order dispersion. This result overcomes

Manuscript received June 12, 1987; revised August 10, 1987.

P. K. A. Wai, H. H. Chen, and Y. C. Lee are with the Laboratory for Plasma and Fusion Energy Studies, University of Maryland, College Park, MD 20742.

C. R. Menyuk is with the Department of Electrical Engineering, University of Maryland, College Park, MD 20742.

IEEE Log Number 8717796.

a major hurdle for the new scheme. If long period axial variations are eliminated by carefully controlling the manufacturing process of the fiber, solitons propagate in the neighborhood of a rapidly fluctuating zero dispersion point.

The present paper is arranged as follows. The results in the ideal case with no axial variations are reviewed in Section II. In Section III, the equation governing the evolution of the pulse envelope at the zero dispersion point, including the effect of axial inhomogeneity, is introduced. The magnitude and correlation length of the variations in a fiber are discussed. In Section IV, we introduce scale lengths corresponding to different physical effects. A multiple length scale expansion, based on ordering the different scale lengths, is used to demonstrate soliton propagation near the fluctuating zero dispersion point. In Section V, the equation of motion is integrated numerically. The effects of different correlation lengths with different amplitudes are studied in detail by assuming an axial variation which consists of a single Fourier mode. Finally, random fluctuation of the zero dispersion point is simulated by a Gaussian modulated Fourier series with randomly chosen frequencies.

II. Ideal Case

Using the slow-varying envelope approximation, we find that the pulse envelope of the electric field, assuming no axial inhomogeneity, satisfies the equation

$$i\left(\frac{\partial\phi}{\partial z} + \gamma\phi + k'\frac{\partial\phi}{\partial t}\right) - \frac{1}{2}k''\frac{\partial^2\phi}{\partial t^2} - \frac{1}{6}ik'''\frac{\partial^3\phi}{\partial t^3} + \frac{\omega_0 n_2}{2c}|\phi|^2\phi = 0 \tag{1}$$

where n_2 is the Kerr coefficient, k is the propagation constant, $k' = \partial k/\partial\omega$, $k'' = \partial^2 k/\partial\omega^2$, $k''' = \partial^3 k/\partial\omega^3$, γ^{-1} is the attenuation length, and ω_0 is the carrier frequency. The propagation constant and its derivatives are independent of the axial coordinate z. At the zero dispersion point, $k'' = 0$. Letting τ equal the pulse width, (1) is reduced to dimensionless form using the following transformation:

$$s = (t - k'z)/\tau \tag{2}$$

$$\xi = |k'''|z/\tau^3 \tag{3}$$

$$q = \left|\frac{\omega_0 n_2 \tau^3}{2ck'''}\right|^{1/2}\phi \tag{4}$$

to

$$i\frac{\partial q}{\partial\xi} - i\frac{1}{6}\frac{\partial^3 q}{\partial s^3} + |q|^2 q = i\Gamma q \tag{5}$$

where $\Gamma = \gamma\tau^3/k'''$. In subsequent discussion, the effect of attenuation on the fiber is ignored, and Γ is set to zero. For hyperbolic secant initial conditions, $q(0, s) = A_0 \operatorname{sech}(s)$, the soliton forms over a length $\xi = 10/A_0^2$ when $A_0 > 1.5$ and somewhat more quickly at lower values of A_0. Hence, attenuation will not affect the soliton's emergence, as long as $\Gamma < A_0^2/10$. If Raman amplification is used, then it may be possible to bypass this constraint on A_0.

We look for a soliton of the form

$$q(\xi, s) = \tilde{q}(\theta)\exp(ik_0\xi - i\Omega_0\theta) \tag{6}$$

where $\theta = s - \xi/u$ where u is the speed of the pulse and k_0 and Ω_0 are the shift in normalized wavenumber and frequency of the soliton, respectively. The quantity Ω_0 takes into account the variation in the central frequency near the zero dispersion point. When Ω_0 is large and negative, the soliton is deep inside the anomalous dispersion regime, and the second-order dispersion dominates. The quantity $\tilde{q}(\theta)$ can then be determined from the nonlinear Schrödinger equation with third-order dispersion being treated as a perturbation. Subsitution of (6) into (5) yields

$$-i\frac{1}{6}\frac{d^3\tilde{q}}{d\theta^3} - \frac{1}{2}\Omega_0\frac{d^2\tilde{q}}{d\theta^2} + i\left(\frac{1}{2}\Omega_0^2 - \frac{1}{u}\right)\frac{d\tilde{q}}{d\theta} - \left(k_0 - \frac{1}{6}\Omega_0^3\right)\tilde{q} + |\tilde{q}|^2\tilde{q} = 0. \tag{7}$$

The boundary conditions for $\tilde{q}(\theta)$ is taken to be

$$\tilde{q}(\theta) \to 2a_0 e^{-\sigma|\theta|}, \quad \text{as } |\theta| \to \infty \tag{8}$$

where a_0 and σ are real constants. Equations (7) and (8) are solved numerically using the shooting method. It is found that solutions are possible if a_0, σ, and Ω_0 are chosen such that

$$a_0^2 \approx \left[1 - \frac{5}{6}\left(\frac{\sigma}{\Omega_0}\right)^2\right]\sigma^2|\Omega_0| \tag{9}$$

$$0 > \frac{\sigma}{\Omega_0} > -0.24. \tag{10}$$

Fig. 1 plots the solutions for the amplitude $|\tilde{q}(\theta)|$ and the normalized instantaneous frequency $-\mathrm{Im}\{d \ln[\tilde{q}(\theta)]/d\theta\}$ for $\sigma = 1$ and $\Omega_0 = 4.5$. We then verify the soliton's existence by integrating (5) numerically using the split-step Fourier method with the solution of (7) and (8) as the initial profile. It is observed that the pulse propagates without change in shape.

The bandwidth of the soliton equals σ, so that in actual physical quantities, (10) can be written as

$$(2t_0)\Delta\lambda > 6\,(\mathrm{nm})(\mathrm{ps}) \tag{11}$$

where $2t_0$ is FWHM and $\Delta\lambda$ is the shift in wavelength towards the anomalous regime. For a given pulse width, (11) imposes a lower limit on $\Delta\lambda$. The peak power P_0 required to launch a soliton is

$$P_0(2t_0)^3 \approx \frac{\epsilon n_0 c\lambda k'''}{\pi n_2}\left|\frac{\Omega_0}{\sigma}\right|S \tag{12}$$

where $\epsilon = 8.85 \times 10^{-12}$ F/m, c is the speed of light, and S is the effective core area. For pure silica fiber, the material dispersion vanishes at $\lambda_0 = 1.27\ \mu$m. If we take $k''' = 0.08\,(\mathrm{ps})^3/\mathrm{km}$, $n_0 = 1.5$, $n_2 = 1.22 \times 10^{-22}\,(\mathrm{m/V})^2$,

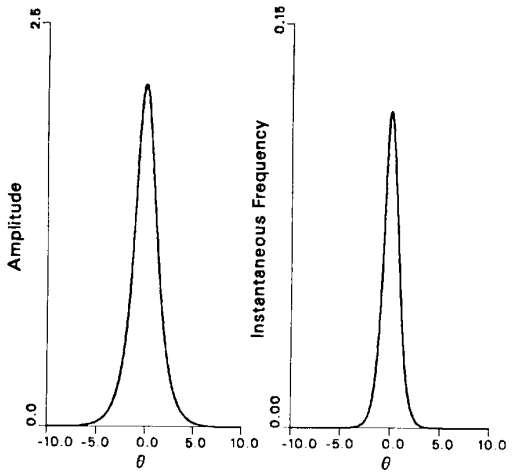

Fig. 1. The amplitude and instantaneous frequency of a soliton of the ideal equation near the zero dispersion point. The bandwidth $\sigma = 1$ and frequency shift $\Omega_0 = 4.5$.

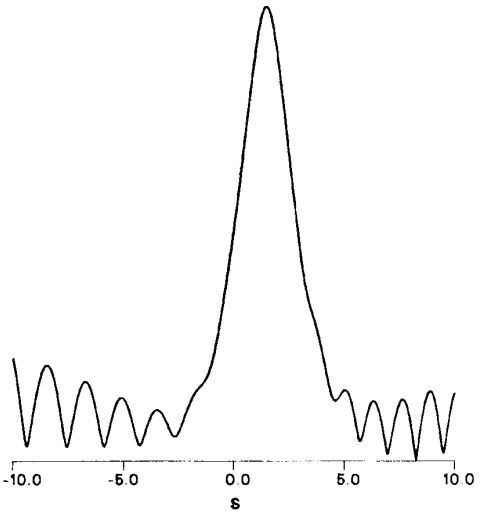

Fig. 2. The pulse amplitude for a hyperbolic secant initial profile with $A_0 = 2$ at $\xi = 10$. The soliton peak is surrounded by a pedestal consisting of dispersive waves.

and $S = 20\ \mu m^2$, (12) and (10) together give

$$P_0(2t_0)^3 \geq 0.16\ \mathrm{W(ps)}^3. \tag{13}$$

Equations (10) and (13) form the basis for the design of a high bit-rate optical communication system in the vicinity of λ_0. If the pulse width is 1 ps, $\Delta\lambda = 0.01\ \mu m$, and the peak power required is only 0.16 W. For a 2 ps pulse, $\Delta\lambda = 0.005\ \mu m$ and only 20 mW peak power is required. The wavelength shift is automatically produced by the fiber as long as the initial center frequency of the pulse is at or slightly below the zero dispersion point and should be relatively insensitive to variations of the zero dispersion point along the fiber length. For a 2 ps pulse, the dispersion and the nonlinearity only become effective over 100 km, and the use of solitons is only of interest over greater propagation lengths. At these long lengths, this approach must be used in conjunction with Raman amplification.

An important property of nonlinear Schrödinger equation solitons is that they emerge from arbitrary initial profiles as long as a threshold condition is met. As a consequence, it is possible to experimentally observe solitons when neither the initial pulse amplitude nor the initial pulse shape corresponds to a pure soliton. To determine whether a similar property holds for the solitons of (5), we integrated (5) numerically, taking $q(0, s) = A_0$ sech (s) as our initial conditions, corresponding to pulses with the central wavelength at the zero dispersion wavelength λ_0. The initial amplitude A_0 is varied and the subsequent pulse evolution is followed up to $\xi = 15$. We also investigated Gaussian pulses in a similar fashion. The evolution is qualitatively similar in both cases, although solitons emerge over a length about a factor of two larger in the latter case. The step size is halved, the node spacing is halved, and the simulation region is doubled in selected cases to ensure accuracy of the results. In general, dispersive waves appear as multiple peaks at the leading edge of the pulse (a consequence of $k''' > 0$; for the opposite sign, the dispersive waves would appear at the trailing edge) and eventually separate from the main peak. The normalized distance required for the separation decreases with increasing amplitude. The peak that is left behind is a soliton. Both the soliton and the dispersive waves move in the forward direction. Fig. 2 shows the pulse amplitude for a hyperbolic secant initial profile with $A_0 = 2$ at $\xi = 10$. The dispersive waves and the soliton part can be readily identified. The evolution into a soliton and dispersive waves is more obvious in the frequency spectrum. The initial spectrum splits into two peaks at either side of the zero dispersion frequency ω_0. The peak in the anomalous regime corresponds to the soliton part, while the peak in the normal regime corresponds to the dispersive wave component. The interaction between the two components shifts part of the pulse from the normal to the anomalous regime. The soliton contains approximate 60 percent of input power for all the cases considered. Fig. 3 shows the two-peak structure of the spectrum for $A_0 = 2$ at $\xi = 2$. The shift in frequency of the soliton and dispersive waves from ω_0 is different, with the latter about 1.7 times larger than the former. Since the group delay $(1/v_g)$ is proportional to the square of the normalized frequency shift, the dispersive wave component travels faster and breaks away from the soliton. Fig. 4 plots the frequency shift of the solitons which emerge at different values of A_0. This figure shows that the shift varies almost linearly with A_0. Hence, the dispersive wave component separates from the soliton at a shorter distance for larger A_0.

III. Axial Inhomogeneity

In this section, we discuss the effect of variation of fiber parameters, particularly the chromatic dispersion, along the fiber axis. The chromatic dispersion or, more precisely, the coefficient of second-order dispersion (k''), is composed of material dispersion and waveguide disper-

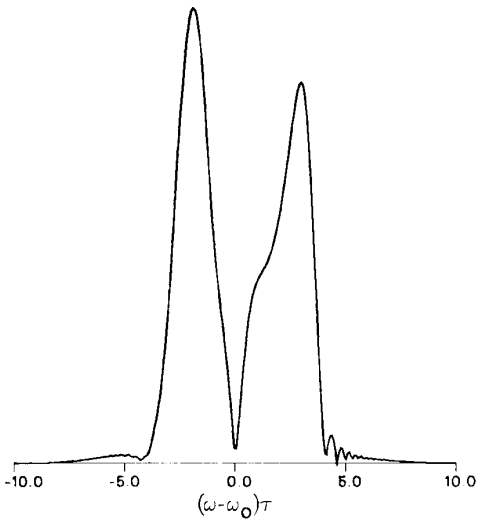

Fig. 3. The frequency spectrum at $\xi = 2$ for $A_0 = 2$. The peak in the anomalous regime corresponds to the soliton, while that in the normal regime corresponds to dispersive waves.

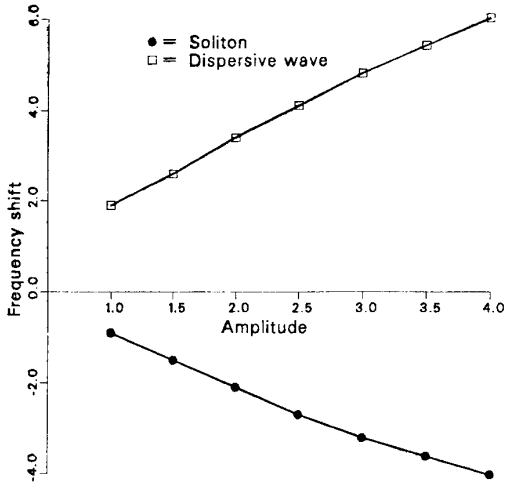

Fig. 4. The frequency shifts of the solitons and the dispersive waves plotted versus initial amplitudes of hyperbolic secant profiles for the ideal case.

sion. The former depends only on the refractive index and the operating wavelength, while the latter is a function of fiber parameters. The wavelength at which the material and waveguide dispersion balance each other is called the zero dispersion point. For an ideal fiber, its parameters are assumed to be perfectly axial-invariant; hence, the zero dispersion point is constant. In practice, the waveguide parameters, for example, the core radius and the index difference between the core and the cladding in a step-index fiber, fluctuate along the fiber. Consequently, for a carrier wavelength, cancellation between the two types of dispersion over the whole length of the fiber is not possible. In other words, the zero dispersion point fluctuates due to the axial variations. A pulse launched at the zero dispersion wavelength at one point is subjected to both normal and anomalous dispersion when it travels along the fiber.

Equation (1) is, therefore, no longer a valid model of the situation. It has to be modified to include the effect of axial variations. We assume that the inhomogeneity along the axial direction is small so that $|\lambda\partial \ln(\epsilon)/\partial z| \ll 1$ where λ is the carrier wavelength and ϵ is the dielectric constant. In this case, (1) holds except that the coefficients k', k'', and k''' are now dependent on the axial coordinate due to the fluctuation. More important, the chromatic dispersion k'' cannot be set to zero as in the case of an ideal fiber. Since the variations of k''' are small compared to their average magnitude, they can safely be ignored. Equation (1) is again normalized by using the transformation in (2), (3), and (4). Equation (2) for the time variable transformation is modified to

$$s = \left[t - \int^{z} k'(\tilde{z})\, d\tilde{z}\right]\Big/\tau \tag{14}$$

to account for the axial dependence of the group delay $k'(z)$. If the group delay is independent of z, (14) reduces to the original equation. The normalized equation at the zero dispersion point including the effect of axial inhomogeneity is given by

$$i\frac{\partial q}{\partial \xi} - \frac{1}{2}f(\xi)\frac{\partial^2 q}{\partial s^2} - i\frac{1}{6}\frac{\partial^3 q}{\partial s^3} + |q|^2 q = 0 \tag{15}$$

where

$$f(\xi) = \tau k''/k'''.$$

Apart from the modification of the group delay, the effect of axial variations is to reintroduce the second-order dispersion term. Its coefficient takes on both positive and negative values. Equation (15) forms the basis of the follow analysis. Although (15) is obtained using heuristic arguments, it can be derived rigorously starting from Maxwell's equations and using the reductive perturbation method developed by Taniuti *et al.* [7], [8].

We proceed to estimate the magnitude of the variation of the second-order coefficient. An explicit expression for the coefficient can be obtained from the exact derivation. For a step-index fiber, assuming a transverse electric field, the variation of the second-order coefficient at the zero dispersion point has been estimated to be [9]

$$\delta k'' = -4\frac{\delta\Delta n}{\Delta n} - 12\frac{\delta a}{a}\left((\text{ps})^2/\text{km}\right) \tag{16}$$

where a is the core radius, Δn is the index difference, and $\delta\Delta n$ and δa are the corresponding fluctuations. For example, a variation of the core radius by 1 percent [6] and a negligible variation of the index difference [10] would give a variation of $\pm 0.12\ (\text{ps})^2/\text{km}$ in chromatic dispersion. The magnitude of the variations of the normalized coefficient is given by $|f(\xi)| = 1.5\tau\ (\text{ps})$. For a 1 ps pulse, $|f(\xi)| = 1.5$. Therefore, the contribution from the second-order dispersion term in (15) is not small.

Another important parameter governing the axial vari-

ation is the correlation length of the fluctuations. The outer diameter of an optical fiber can be controlled carefully in the drawing process through a feedback controlled system using nondestructive and noncontacting measurement methods such as the scanning beam technique or the forward scattering method [6], [11]. On the other hand, the core diameter cannot be monitored directly in the pulling process. If one assumes that the ratio of the core to the cladding diameter is strictly maintained, the variations in the core diameter are then proportional to those in the outer diameter. The diameter variations can originate from vibration in the drawing machine, from thermal instabilities such as turbulent cooling of the hot gases, or long-term temperature drift. They can also result from mechanical problems such as variations in a lead screw that is feeding the preform, or from eccentric drawing drums, or from some cogging effect in a gear mechanism [6]. They give rise to correlation lengths on the order of meters or less. In addition, long periodic variations can result from composition variations in the preform caused by the fabrication process. Variations in the index difference also arise from the fabrication process and possible diffusion of dopant materials. The correlation length in normalized coordinates is given by $L_c = k''' l_c/\tau^3 = 0.1 \times l_c\ (\text{km})/\tau^3\ (\text{ps})$ where L_c is the normalized correlation length and l_c is the correlation length in physical unit. For a 1 ps pulse and $l_c \sim 1$ m, $L_c \sim 10^{-4}$. The normalized correlation length can, therefore, be very short. We are going to demonstrate that if the correlation length of axial variations is sufficiently short, soliton propagation is possible even when the strength of the fluctuation $|f(\xi)|$ is large. The axial variation has almost no effect on the evolution characteristics.

IV. Scale Lengths

First, we consider the different length scales which play a role in the fiber. Two of these are the carrier wavelength and the core radius. They are of the same order, and are much smaller than any other length scales in the fiber.

We now introduce the concept of characteristics dispersion length, which is defined as the distance at which the effect of dispersion becomes important. There are two different characteristic dispersion lengths, corresponding to the second- and the third-order dispersion. The second-order dispersion length is defined as $l_s = \tau^2/|k''|$, and the third-order dispersion length is given by $l_t = \tau^3/|k'''|$. In the case of interest in this paper, the second-order dispersion length l_s fluctuates between a minimum value $l_{sm} = \tau^2/|k''|_{\max}$, corresponding to the maximum value of k'', and infinity, corresponding to $k'' = 0$. Equation (15) is normalized to the third-order dispersion length. Notice that the normalized second-order coefficient of (15) is the ratio between the third-order and the second-order dispersion length $f(\xi) = l_t/l_s$.

We now look at the parameter regimes where (15) can be approximated by (5), the ideal equation. In the regime where the third-order dispersion length is much shorter than the minimum second-order dispersion length, i.e., $l_t \ll l_{sm}$ or, equivalently, $f(\xi) \ll 1$, the effect of axial inhomogeneity can be treated as a small perturbation. The evolution characteristics of the fiber are not changed significantly in this case. Soliton propagation near the fluctuating zero dispersion point is not affected. However, this regime corresponds to a very stringent control on the fiber parameters such as the core radius. For example, if one requires that $|f(\xi)| = 0.01$ for a 1 ps pulse, the tolerance on the core radius would be 0.01 percent, a highly unrealistic demand. This regime can also be achieved by using very short pulses ($\tau \ll 1$), but then the higher order nonlinear effects which are ignored in (15) would become important. Equation (15) would no longer be valid. Another parameter regime of interest is when the third-order dispersion length is much shorter than the correlation length $l_t \ll l_c$. The variation of the second-order dispersion with the axial coordinate is very slow and can be assumed to be constant over the dispersion length. Therefore, if the carrier wavelength is chosen initially at $k'' \approx 0$, the chromatic dispersion would stay small for a long time. The solitons would adjust adiabatically to the slowly changing dispersion. However, for a 1 ps pulse, the third-order dispersion length l_t is on the order of kilometers. This implies a correlation length on the order of hundreds of kilometers, an unrealistic number for most fibers.

The most interesting, and also physically important, regime of parameters is when the correlation length is much shorter than both the minimum second-order dispersion length and the third-order dispersion length, i.e., $l_c \ll l_{sm}$ and $l_c \ll l_t$. Soliton propagation in this regime is possible, and its evolution characteristics are similar to that of the ideal case. This result might seem a bit surprising because the minimum second-order dispersion length can be very small so that the magnitude of the axial variations ($|f(\xi)|$) is very large. However, since the correlation length is assumed to be much shorter than the minimum second-order dispersion length, the coefficient $f(\xi)$ changes sign many times in a distance of length l_{sm}. In other words, the zero dispersion point varies about the zero value so fast that its effect is averaged out, and the pulse is governed by the weaker third-order dispersion.

To illustrate the above arguments, let us assume the normalized second-order coefficient to be of the following form:

$$f(\xi) = \frac{1}{\delta}\, g\left(\frac{\xi}{\Delta}\right) \tag{17}$$

where $\Delta = l_c/l_t$, $\delta = l_{sm}/l_t$, and $g(\xi)$ is a function with a maximum amplitude of one. Let us assume that the correlation length is much shorter than the minimum second-order dispersion length. For example, let $\Delta = \delta^2$. Since $\Delta \ll \delta \ll 1$, the criteria $l_c \ll l_{sm}$, and $l_c \ll l_t$ is satisfied. The variation of the second-order dispersion in this case is both large and rapid. We now apply the method of multiple length scale expansions [12] to (15) and (17). We first assume that the envelope $q(\xi)$ depends on both

the fast (η_0) and the slow (η_1) variables, defined as

$$\eta_0 = \xi/\delta^2 \tag{18}$$

$$\eta_1 = \xi. \tag{19}$$

Substitution of (18) into (15) and (17) gives

$$\frac{i}{\delta^2}\frac{\partial q}{\partial \eta_0} + i\frac{\partial q}{\partial \eta_1} - \frac{1}{2\delta}g(\eta_0)\frac{\partial^2 q}{\partial s^2} - i\frac{1}{6}\frac{\partial^3 q}{\partial s^3} + |q|^2 q = 0. \tag{20}$$

We then write $q(\eta_0, \eta_1, s)$ as a series in the small parameter δ:

$$q(\eta_0, \eta_1, s) = \sum_{n=0}^{\infty} \delta^n q^{(n)}(\eta_0, \eta_1, s). \tag{21}$$

We substitute (21) into (20) and collect terms at the same order of δ. At order δ^{-2}, we have

$$i\frac{\partial q^{(0)}}{\partial \eta_0} = 0. \tag{22}$$

Therefore, $q^{(0)}$ is independent of the fast variable. Its slow variable dependence is determined at higher order. At order δ^{-1}, we have

$$i\frac{\partial q^{(1)}}{\partial \eta_0} - \frac{1}{2}g(\eta_0)\frac{\partial^2 q^{(0)}}{\partial s^2} = 0 \tag{23}$$

from which we obtain

$$q^{(1)} = -i\bar{g}(\eta_0)\frac{\partial^2 q^{(0)}}{\partial s^2} + \bar{q}^{(1)}(\eta_1, s) \tag{24}$$

where $\bar{g}(\eta_0) = (1/2)\int^{\eta_0} g(\eta)\, d\eta$, and $\bar{q}^{(1)}(\eta_1, s)$ is a function of the slow variable only. At order 1, we have

$$i\frac{\partial q^{(2)}}{\partial \eta_0} + i\frac{\partial q^{(0)}}{\partial \eta_1} - \frac{1}{2}g(\eta_0)\frac{\partial^2 q^{(1)}}{\partial s^2} - i\frac{1}{6}\frac{\partial^3 q^{(0)}}{\partial s^3} + |q^{(0)}|^2 q^{(0)} = 0 \tag{25}$$

from which we obtain the fast time dependence of $q^{(2)}$:

$$q^{(2)}(\eta_0, \eta_1, s) = i\left\{ i\frac{\partial q^{(0)}}{\partial \eta_1} - i\frac{1}{6}\frac{\partial^3 q^{(0)}}{\partial s^3} + |q^{(0)}|^2 q^{(0)} \right\}\eta_0 - \frac{1}{2}\bar{g}^2\frac{\partial^4 q^{(0)}}{\partial s^4} - i\bar{g}\frac{\partial^2 \bar{q}^{(1)}}{\partial s^2} + i\bar{q}^{(2)} \tag{26}$$

where $\bar{q}^{(2)}$ is only a function of the slow variables. From (26), we see that the function $q^{(2)}(\eta_0, \eta_1, s)$ grows linearly with the fast variable η_0. At a distance of $\eta_0 \sim 1/\delta^2$ or $\xi = 1$, i.e., the third-order dispersion length, $q^{(0)}$ and $q^{(1)}$ have the same order of magnitude. The expansion in (21) therefore becomes invalid. In order to extend the region of validity of the series expansion, we eliminate the secularity by demanding that its coefficient be zero. Hence,

$$i\frac{\partial q^{(0)}}{\partial \eta_1} - i\frac{1}{6}\frac{\partial^3 q^{(0)}}{\partial s^3} + |q^{(0)}|^2 q^{(0)} = 0 \tag{27}$$

which is exactly the same as (1). Therefore, at leading order, the pulse evolves as if there is no axial variation. Similarly, at the next order of δ, we find that $\bar{q}^{(1)}(\eta_1, s)$ is governed by the linearized form of (27). To first order in δ, the pulse envelope is given by

$$q(\eta_0, \eta_1, s) = q^{(0)}(\eta_1, s) + \delta\left\{ -i\bar{g}(\eta_0)\cdot\frac{\partial^2 q^{(0)}}{\partial s^2} + \bar{q}^{(1)}(\eta_1, s)\right\}. \tag{28}$$

The modification in the pulse envolpe due to the axial variation of the fiber only appears at the first order in the small parameter δ, even though the amplitude of the fluctuation of the normalized chromatic dispersion is very large ($\sim 1/\delta$). Further calculations show that the secularities which appear at higher order can be eliminated in a similar fashion. Equation (28) has a range of validity which is at least of order $\xi \sim \delta^{-2}$. In the above argument, the assumption $\Delta = \delta^2$ is not essential. The derivation remains valid as long as $\Delta \ll \delta$. In fact, numerical simulations show that soliton propagation is still possible even when $l_c \sim l_{sm}$. Our estimates are conservative because we overestimate the effect of the second-order dispersion length by using the maximum second-order dispersion.

V. Numerical Results

In this section, (15) is integrated numerically using different functions for the normalized second-order coefficient $f(\xi)$. In practice, the fiber variations are very complex. If the drawing process is random or random with some deterministic components, the waveform representing the axial variation can be Fourier decomposed. We first study the case where $f(\xi)$ consists of a single Fourier component, i.e., $f(\xi) = f_0 \sin(\kappa\xi + \chi)$ where f_0, κ, and χ are constant parameters. This model allows us to study the effect of different amplitudes and fluctuation lengths in detail. The initial pulse is chosen to be 2 sech (s) in all cases that we report here. This choice is somewhat arbitrary; however, if the initial pulse amplitude is too weak ($\lesssim 1$), the pulse will not evolve into a soliton, and if the initial amplitude is too large ($\gtrsim 4$), the pulse may break up into multiple solitons. Studies that we have carried out on Gaussian waveforms yield qualitatively similar results.

The amplitude and the wavenumber of the fluctuations are varied between 10^{-2} and 10^2. The equation is integrated up to $\xi = 15$. While this represents 10^3 cycles if $\kappa = 500$, it is only one-tenth of a cyle for the case $\kappa = 0.05$. We do not integrate past $\xi = 15$ because with a pulse width on the order of 1 ps, $\xi = 15$ already represents 200 km, and other effects such as dissipation have to be taken into account. The results obtained verify the analysis in

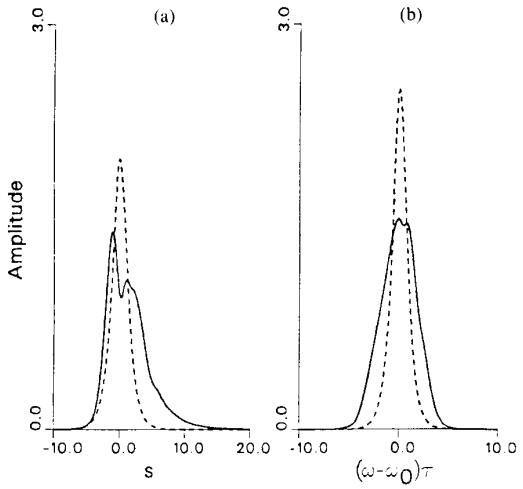

Fig. 5. (a) The pulse shape of an initial profile 2 sech (s) at $\xi = 1$; the axial inhomogeneity is given by $f_0(\xi) = 10 \sin(0.4\xi)$. (b) The corresponding frequency spectrum. The pulse is broadened and distorted. There is no splitting in the frequency spectrum. The initial pulse is shown in dashed line for comparison.

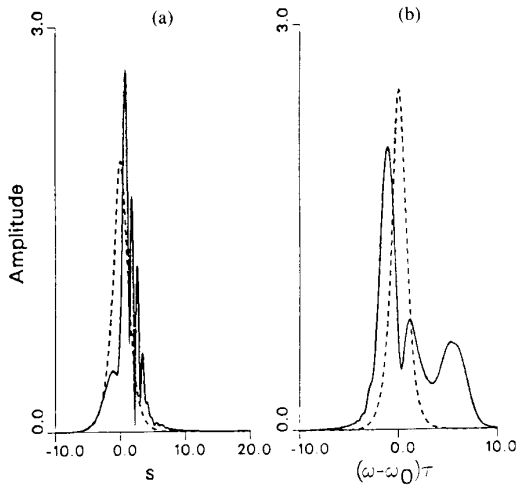

Fig. 6. (a) The pulse shape of an initial profile 2 sech (s) at $\xi = 1$; the axial inhomogeneity is given by $f_0(\xi) = -10 \sin(0.4\xi)$. (b) The corresponding frequency spectrum. The soliton can be identified in the negative part of the frequency spectrum. The initial pulse is shown in dashed line for comparison.

Section IV. When f_0 is small ($\lesssim 0.1$), the evolution of the initial pulse is essentially the same at all wavenumbers κ. If the fluctuation length is very long ($\kappa \lesssim 0.1$), the evolution is sensitive to the initial phase χ. For example, if $\chi = 0$, the pulse broadens for large f_0 and no soliton emerges. In this case, the zero dispersion point moves towards longer wavelengths and the pulse is in the normal regime. In this regime, the nonlinearity and the dispersion both work to broaden the pulse. If $\chi = \pi$, the zero dispersion point moves towards a shorter wavelength, leaving the pulse in the anomalous dispersion regime. The pulse first contracts due to the interplay between the anomalous dispersion and the nonlinearity. A soliton is formed. As the strength of the dispersion increases, the pulse begins to broaden and finally disperses away. Fig. 5(a) shows the pulse shape for $f_0 = 10$, $\kappa = 0.4$, $\chi = 0$ after $\xi = 1$, and Fig. 5(b) gives the corresponding frequency spectrum. The pulse has broadened considerably, and there is no splitting in the frequency spectrum. The initial pulse 2 sech (s) is shown in the dashed lines for comparison. When $\chi = \pi$, as shown in Fig. 6(a) and 6(b), the soliton peak is in the negative part of the spectrum. When ξ increases, the soliton starts to broaden due to an increase in chromatic dispersion. When the variations are very short ($\kappa \gtrsim 10$), the initial phase is not essential, and the propagation characteristics are almost indistinguishable from those of the ideal case. We find that solitons propagate even in a regime where the analytic arguments are not applicable, i.e., when the fluctuations amplitude is large but the correlation length is not short enough. For example, in the case of $f_0 = 100$ and $\kappa = 40$, the pulse evolves differently; it takes $\xi = 6$ for the two-peak structure to develop in the frequency spectrum, while it takes only $\xi = 1.5$ for the ideal case. However, a soliton with a somewhat different amplitude and pulsewidth finally emerges.

We then simulate the axial fluctuations by using the following series [13], [14]:

$$f(\xi) = f_0 \sum_{n=0}^{N} \exp(-\alpha r_n^2) \sin(\kappa_n \xi + \chi_n) \quad (29)$$

where $\kappa_n = \kappa_0 - r_n \Delta\kappa$, r_n is a random number $-1 \leq r_n \leq 1$, and χ_n is random phase. Equation (29) represents a finite Fourier series with N wavenumbers randomly distributed between two cutoffs at $\kappa_0 \pm \Delta\kappa$. The cutoffs are introduced because physically there are neither very long nor very short correlations in a fiber. The magnitude of the Fourier components are Gaussian modulated with the maximum value f_0 at κ_0. The half width of the modulation is controlled by the parameter α. Fig. 7 shows one realization of the Fourier component distribution and the corresponding amplitudes for the case $\alpha = 10$, $N = 40$, $f_0 = 10$, $\kappa_0 = 400$, and $\Delta\kappa = 400$. Fig. 8 gives the corresponding variations of $f(\xi)$ as a function of ξ.

The parameter $\Delta\kappa$ is chosen to be κ_0 for all the cases reported here. It cuts off short wavelength fluctuation, but does not affect the long wavelength variations. When f_0 is small ($\lesssim 0.1$), the results again resemble those of the ideal case for all center wavenumbers κ_0, modulation bandwidths α, and numbers of Fourier components N; solitons emerge from the initial pulse. If f_0 is not small ($\gtrsim 10$), the results divide roughly into two categories—those of large and small α. If the spectrum of the axial fluctuation is sharp, i.e., α is large, the evolution of the initial pulse is similar to the results where there is only a single Fourier component with amplitude f_0 and wavenumber κ_0. Solitons emerge if $\kappa_0 \gg f_0$. For example, Fig. 9 gives the pulse amplitude at $\xi = 10$ for the axial variation shown in Figs. 7 and 8, i.e., the case with $\alpha = 10$, $N = 40$, $f_0 = 10$, $\kappa_0 = 400$, and $\Delta\kappa = 400$. It is the same as the result shown in Fig. 2 for ideal case. The variation of the evolution characteristics among different realizations of

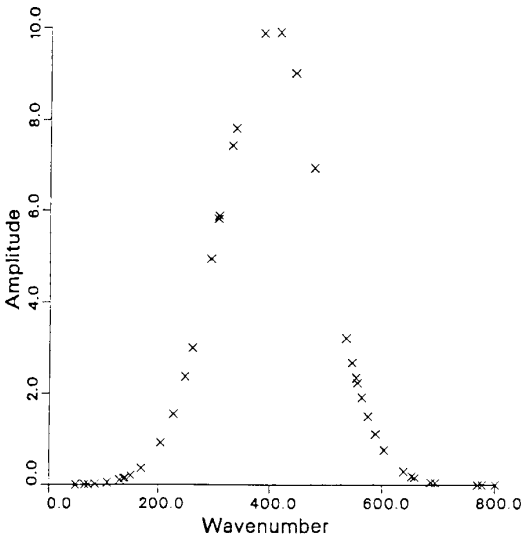

Fig. 7. One realization of the spectrum of the axial inhomogeneity with 40 Fourier components, modulation bandwidth $\alpha = 10$, center wavenumber $\kappa_0 = 400$, $f_0 = 10$, and cutoff wavenumbers amplitude at 0 and 800.

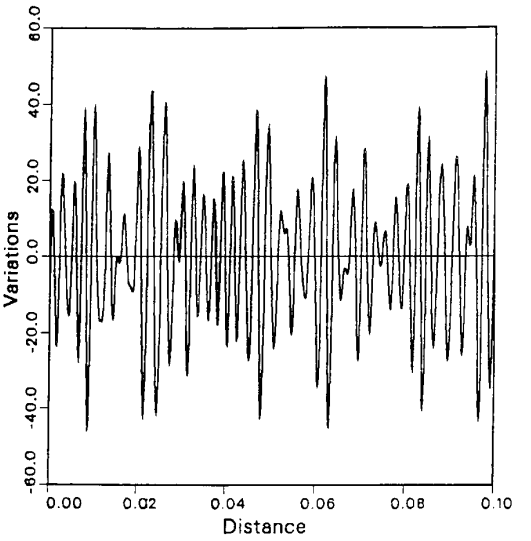

Fig. 8. The axial variation $f_0(\xi)$ as a function of ξ for the spectrum shown in Fig. 7.

the Gaussian-modulated random wavenumbers are small. We have used both 40 and 100 Fourier modes; there is no significant change in behavior. When the axial variation has a broad spectrum (α small), there are relatively large contributions from the long wavelength components. In this case, the results differ from the case where only a single component at the central wavenumber κ_0 is kept. The evolution of the pulse is dominated by the long wavelength components and their initial phases. Generally, the initial pulse broadens and no soliton emerges.

VI. Conclusions

In the case of an ideal fiber which is axially uniform, we have shown that it is possible to launch solitons from

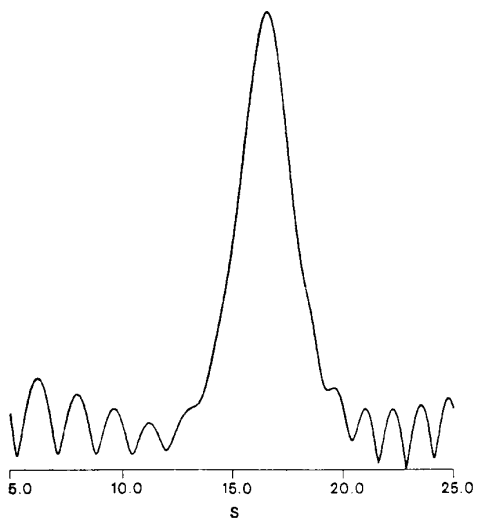

Fig. 9. The pulse amplitude of an initial profile 2 sech (s) at $\xi = 10$. The axial variation is given by that shown in Figs. 7 and 8 for $N = 40$, $\alpha = 10$, $\kappa_0 = 400$, $f_0 = 10$, and $\Delta\kappa = 400$. The soliton pulse is identical to that shown in Fig. 2 for the ideal case.

pulses near the zero dispersion wavelength of single-mode optical fibers. These solitons have central frequencies downshifted into the anomalous dispersion regime. The size of the downshift increases with the initial pulse amplitude. For a given pulsewidth, we have determined the minimum power required to launch a soliton. This power is substantially lower than that required to launch solitons in the experiments to date. We have also shown that solitons will emerge from arbitrary initial profiles and amplitudes above the minimum power threshold. If the effect of axial inhomogeneity is included, we note that the variations generally have large amplitudes. A physically important regime of parameters has been found analytically, and extended by results from numerical simulations in which soliton propagation is nonetheless possible. If the correlation length of the axial inhomogeneity is short compared to the second-order and the third-order dispersion lengths, the effect of the fluctuations is averaged out. The evolution characteristics of the pulse are then described by the ideal equation.

References

[1] A. Hasegawa and F. Tappert, "Transmission of stationary nonlinear pulses in dispersive dielectric fibers. I. Anomalous dispersion," *Appl. Phys. Lett.*, vol. 23, pp. 142-144, Aug. 1973.

[2] A. Hasegawa, "Amplication and reshaping of optical solitons in a glass fiber—IV: Use of the stimulated Raman process," *Opt. Lett.*, vol. 8, pp. 650-652, Dec. 1983.

[3] L. F. Mollenauer, R. H. Stolen, and M. N. Islam, "Experimental demonstration of soliton propagation in long fibers: Loss compensated by Raman gain," *Opt. Lett.*, vol. 10, pp. 229-231, May 1985.

[4] L. F. Mollenauer, J. P. Gordon, and M. N. Islam, "Soliton propagation in long fibers with periodically compensated loss," *IEEE J. Quantum Electron.*, vol. QE-1, pp. 157-173, Jan. 1985.

[5] P. K. A. Wai, C. R. Menyuk, H. H. Chen, and Y. C. Lee, "Solitons at the zero dispersion wavelength of single-mode fibers," in *Ultrafast Phenomena V*, (*Springer Series on Chemical Physics, Vol. 46*), G. R. Fleming and A. E. Siegman, Eds. New York: Springer-Verlag, 1986, pp. 65-67, P. K. A. Wai, C. R. Menyuk, H. H. Chen, and Y.

C. Lee, "Solitons at the zero dispersion wavelength of single-mode fibers," *Opt. Lett.*, vol. 12, pp. 628–630, Aug. 1987.
[6] R. E. Jaeger, "Fiber drawing process: Characterization and control," in *Fiber Optics, Advances in Research and Development*, B. Bendow and S. S. Mitra, Eds. New York: Plenum, 1979, pp. 33–53.
[7] T. Taniuti, "Reductive perturbation method and far fields of wave equations," *Progr. Theor. Phys. Suppl.*, vol. 55, pp. 1–35, 1974.
[8] Y. Kodama, "Optical solitons in a monomode fiber," *J. Stat. Phys.*, vol. 39, pp. 597–614, 1985.
[9] L. B. Jeunhomme, *Single-Mode Fiber Optics*. New York: Marcel Dekker, 1983.
[10] R. Stolen, personal communication.
[11] D. Marcuse, *Principles of Optical Fiber Measurement*. New York: Academic, 1981.
[12] A. Nayfeh, *Perturbation Methods*. New York: Wiley, 1973.
[13] S. O. Rice, "Mathematical analysis of random noise," in *Selected Papers on Noise and Stochastic Processes*, N. Wax, Ed. New York: Dover, 1954, pp. 133–294.
[14] P. N. Guzdar, Y. C. Lee, J. F. Drake, and C. S. Liu, "Stimulated Raman scattering with random pump in laser produced plasmas at quarter critical density," Plasma Preprint UMLPF 86-074, Univ. Maryland, College Park, 1986.

P. K. A. Wai, photograph and biography not available at the time of publication.

C. R. Menyuk, photograph and biography not available at the time of publication.

H. H. Chen, photograph and biography not available at the time of publication.

Y. C. Lee, photograph and biography not available at the time of publication.